NEOPLASIA
www.neoplasia.com

Volume 13 Number 1 January 2011 pp. 23–30 23

Activation of Urokinase Plasminogen Activator and Its Receptor Axis Is Essential for Macrophage Infiltration in a Prostate Cancer Mouse Model[1]

Jian Zhang*, Sudha Sud*, Kosuke Mizutani*, Margaret R. Gyetko† and Kenneth J. Pienta*

*Departments of Internal Medicine and Urology, Michigan Center for Translational Pathology and the University of Michigan Comprehensive Cancer Center, Ann Arbor, MI, USA; †Pulmonary and Critical Care Medicine Division, Department of Internal Medicine, Veterans Affairs Ann Arbor Healthcare System and University of Michigan Medical Center, University of Michigan, Ann Arbor, MI, USA

Abstract

Macrophages within the tumor microenvironment promote angiogenesis, extracellular matrix breakdown, and tumor cell migration, invasion, and metastasis. Activation of the urokinase plasminogen activator (uPA) and its receptor (uPAR) axis promotes prostate cancer tumorigenicity, invasion, metastasis, and survival within the tumor microenvironment. The link between macrophage infiltration and the uPA/uPAR axis in prostate cancer development has not been established, although it has been reported that uPA plays a critical role in monocyte and macrophage chemotaxis. In this study, murine prostate cancer RM-1 cells were subcutaneously inoculated into wild-type (WT), uPA$^{-/-}$, and uPAR$^{-/-}$ mice. Tumor volume was significantly diminished in both uPA$^{-/-}$ and uPAR$^{-/-}$ mice compared with WT controls. Greater inhibition of tumor volume was also observed in uPA$^{-/-}$ mice compared with uPAR$^{-/-}$ mice, suggesting the important contribution of stromal-derived uPA to sustain the tumor growth. Immunohistochemical staining revealed that tumors in uPA$^{-/-}$ and uPAR$^{-/-}$ mice displayed significantly lower proliferative indices, higher apoptotic indices, and less neovascularity compared with the tumors in WT mice. Tumors in uPA$^{-/-}$ and uPAR$^{-/-}$ mice displayed significantly less macrophage infiltration as demonstrated by F4/80 staining and MAC3^{+} cell numbers by flow cytometry compared with the tumors from WT mice. These findings suggest that the uPA/uPAR axis acts in both autocrine and paracrine manners in the tumor microenvironment, and activation of uPA/uPAR axis is essential for macrophage infiltration into prostate tumors.

Neoplasia (2011) 13, 23–30

Introduction

The urokinase-type plasminogen activator (uPA) system is composed of uPA, its receptor (uPAR), plasminogen, and plasminogen activator inhibitors. Urokinase-type plasminogen activator is a highly restricted serine protease that converts plasminogen to active plasmin and thus degrades protein components of the extracellular matrix. Binding of uPA to its receptor uPAR initiates pericellular proteolysis and plays critical roles in both physiological and pathological conditions, including cell migration and tissue remodeling in angiogenesis, atherogenesis, and tumor progression and metastasis (see review in Smith and Marshall [1] and Li and Cozzi [2]). The findings that higher plasma or serum levels of uPA correlate with the tumor progression, in particular as a poor prognostic marker in aggressive breast cancer [3,4], bladder cancer [5], gastric cancer [6], as well as prostate cancer [7–9], suggest that the uPA/uPAR axis is a cancer therapeutic target.

It has been demonstrated that human prostate malignant cells express both uPA and uPAR, and levels of uPA and uPAR expression

Abbreviations: ELISA, enzyme-linked immunosorbent assay; TAM, tumor-associated macrophage; uPA, urokinase plasminogen activator; uPAR, urokinase plasminogen activator receptor; WT, wild-type

Address all correspondence to: Jian Zhang, MD, PhD, Department of Internal Medicine and Urology, 1500 E Medical Center Dr, 7310 Comprehensive Cancer Center, Ann Arbor, MI 48109-5946. E-mail: jzhangqi@umich.edu

[1]This work was supported by the Department of Defense PC061231 (J. Zhang) and Prostate Specialized Programs of Research Excellence (J. Zhang); National Institutes of Health PO1 CA093900 (K.J. Pienta), an American Cancer Society Clinical Research Professorship (K.J. Pienta), National Institutes of Health SPORE P50 CA69568 (K.J. Pienta), Cancer Center P30 CA46592 (K.J. Pienta), and Prostate Cancer Foundation (K.J. Pienta).
Received 24 May 2010; Revised 29 September 2010; Accepted 5 October 2010

DOI 10.1593/neo.10728

are upregulated in aggressive prostate cancer cells and stromal cells surrounding the tumor cells and correlate with the metastatic potential of prostate cancer cells [10–15]. The uPA/uPAR axis knockdown by small interfering RNA in prostate cancer PC3 cells resulted in a dramatic reduction of tumor invasion and cell viability and induction of apoptosis [16]. RNAi knockdown of uPA-uPAR expression *in vivo* abrogated tumor growth in an orthotopic prostate cancer tumor model [16]. It was further reported that both tumor-derived uPA and tumor-stroma–induced plasminogen activator inhibitor 1 play important roles in intraosseous metastatic prostate cancer growth [17]. It remains unknown, however, if the stromal-derived uPA defines a permissive microenvironment for prostate cancer development.

The uPA/uPAR axis also plays a critical role in monocyte and macrophage chemotaxis [18,19]. In the tumor microenvironment, inflammatory components present as a large number of infiltrating macrophages (tumor-associated macrophages, TAMs) [20–22]. These TAMs are increasingly recognized as important contributors to cancer progression and metastasis [23]. However, the roles of uPA/uPAR axis in TAMs and prostate cancer progression have not yet been elucidated. In this study, we tested the hypothesis that the uPA/uPAR axis links infiltrating TAMs and prostate cancer development using $uPAR^{-/-}$ and $uPA^{-/-}$ mice.

Materials and Methods

Animals

Wild-type (WT), $uPAR^{-/-}$, and $uPA^{-/-}$ mice, 6 to 8 weeks of age, were used in this study. All mice are immunocompetent in the same background (C57B6/129) [24]. Mice were housed in specific pathogen-free isolation rooms in the University of Michigan Unit for Laboratory Animal Medicine, which is accredited by the American Association for Accreditation of Laboratory Animal Care. All procedures were approved by the animal care committees of the University of Michigan Committee on Use and Care of Animals. $uPAR^{-/-}$, $uPA^{-/-}$ mice, and background-matched control WT mice were generous gifts from Dr P. Carmeliet (Leuven, Belgium). These mice were developed as previously described [25,26]. Genotype of the $uPA^{-/-}$, $uPAR^{-/-}$, and WT mice was confirmed by polymerase chain reaction (PCR) or reverse transcription–PCR analysis as described previously [26,27].

Tumor Cells

The mouse prostate cancer cell line RM-1(H-2b) was obtained from Dr T. Thompson (University of Texas MD Anderson Cancer Center, Houston, TX). This model was generated by transduction of cells with the *ras* and *myc* oncogenes, yielding a poorly differentiated adenocarcinoma [28,29]. Cells were cultured in Dulbecco modified Eagle medium (DMEM) supplemented with 10% FBS.

Tumor Cell Inoculation

Single-cell suspension RM-1 (5000 cells in 100-μl volume of PBS) cells were injected into the right flank of the mice using a 23-gauge needle. The tumor growth was monitored by palpation, and two perpendicular axes were measured using an electronic caliper; the tumor volume was calculated using the formula as described previously [30]: volume = length × width^2 / 2. At the day 15 after tumor cell inoculation, all mice were killed.

Immunohistochemical Staining

Allograft tumors were harvested and placed in 10% formalin, embedded in paraffin, and sectioned at 5-μm thickness. Sections were examined using standard hematoxylin and eosin staining for routine histology. To evaluate the tumor cell proliferation, sections were deparaffinized, rehydrated, and stained with Ki-67 monoclonal antibody (Invitrogen Life Technologies, Carlsbad, CA). To evaluate apoptosis, sections were subjected to terminal deoxynucleotidyl transferase–mediated nick end labeling analysis using the ApopTag Peroxidase *In Situ* Apoptosis Detection Kit (Chemicon International Millipore, Billerica, MA) according to the manufacturer's directions. Both the Ki-67 labeling index and the apoptotic index were calculated as the percentage of positive tumor nuclei divided by the total number of tumor cells examined. At least 1000 tumor cells per specimen were examined in five randomly selected fields by light microscopy (×400). Vessel formation in the allograft tumors was evaluated by an endothelial marker CD31 immunohistochemical staining (Santa Cruz Biotechnology, Santa Cruz, CA). The number of vessels per squared millimeter was counted in five randomly selected fields (×200). To evaluate TAMs in the allograft tumors, F4/80 staining was performed. The F4/80 antibody was purchased from Abcam (Cambridge, MA).

Preparation of Conditioned Medium

RM-1 cells at 2×10^6 were grown in 100-mm tissue culture dishes overnight in cell culture medium and washed twice with PBS. Then, the medium was changed to 1% FBS in DMEM. After 48 hours, the conditioned medium was collected for use in the chemotaxis assay.

Enzyme-Linked Immunosorbent Assay for Murine uPA

The conditioned medium was collected, and uPA levels were measured by enzyme-linked immunosorbent assay (ELISA). Quantikine murine uPA ELISA kits were purchased from Innovative Research (Novi, MI). ELISA was performed according to the manufacturer's instructions.

Flow Cytometric Analysis of TAMs and T Cells in Allograft Tumors

Half of each allograft tumor was harvested and digested with collagenase (Sigma-Aldrich, St Louis, MO) to create a single-cell suspension. Mononuclear cells were collected by layering in Ficoll-Paque centrifuge. Macrophages and T lymphocytes were stained with fluorescein isothiocyanate–conjugated antimouse MAC3 and CD4, CD8 antibodies, respectively (BD Bioscience Pharmingen, San Jose, CA), and their matching isotype controls according to the manufacturer's protocols. The cells were incubated with antibodies for 30 minutes at 4°C and washed with PBS. The percentage of $MAC3^+$, $CD4^+$, and $CD8^+$ population was analyzed using FACSCalibur Flow Cytometer and CellQuest software (BD Bioscience Pharmingen).

Macrophage Chemotaxis Assay

Resident peritoneal macrophages were isolated from the WT, $uPAR^{-/-}$, and $uPA^{-/-}$ mice as previously described [31]. A total of 50,000 macrophages were added to the top well of a 24-well, 8-mm pore size transwell membrane coated with Matrigel (BD Bioscience) in DMEM with 1% FBS. Recombinant monocyte chemotactic protein 1 (MCP-1) was used as a positive control. Plates were incubated for 24 hours at 37°C. After incubation, the top sides of the transwell membranes were thoroughly scraped with a cotton swab, and the bottom surfaces were fixed and stained with Diff-Quick Stain Set according to the manufacturer's recommendations (Dade Behring, Newark,

DE). Transwell membranes were mounted, and macrophages were counted. Experimental groups were performed in triplicate, and counts represent an average, across the three replicates, of five random fields counted at ×200 magnification.

Statistical Analysis

Results were reported as mean ± SD or mean ± SE, indicated in the figure legends. The calculations were done using the StatView system (Abacus Concepts, Berkeley, CA). Changes of each parameter among the groups were initially analyzed by one-way analysis of variance. Differences between WT and KO mice were then analyzed by Student's *t* test. Differences with $P < .05$ were determined as statistically significant.

Results

Murine RM-1 Tumor Was Diminished in uPA$^{-/-}$ and uPAR$^{-/-}$ Mice Compared with the WT Animals

To determine the tumor growth in uPA$^{-/-}$ and uPAR$^{-/-}$ mice compared with the WT animals, the RM-1 cells were inoculated subcutaneously into the mice deficient of either uPA or uPAR and WT counterparts. The tumor volume was monitored at 3-day intervals [29,32]. RM-1 tumors in WT mice grew rapidly and reached a mean size of 500 mm^3 on day 15 after tumor cell inoculation. In contrast, tumor growth in uPA$^{-/-}$ and uPAR$^{-/-}$ mice had a significantly slower growth rate reaching a mean size of 100 and 182 mm^3, respectively, on day 15 (Figure 1). The tumor volume in both uPA$^{-/-}$ and uPAR$^{-/-}$ mice at days 9, 12, and 15 was significantly diminished compared with the tumor volume in WT mice. In addition, a nonsignificant trend toward inhibition of tumor growth in uPA$^{-/-}$ mice was observed compared with uPAR$^{-/-}$ mice on day 12, and a statistically significant inhibition of tumor growth was achieved in uPA$^{-/-}$ mice compared with uPAR$^{-/-}$ mice at day 15 (Figure 1). All organs including liver, lung, brain, spleen, kidney, femurs, tibiae, and vertebrae were sectioned and examined by hematoxylin and eosin staining. Metastatic tumors were not observed in these organs (data not shown).

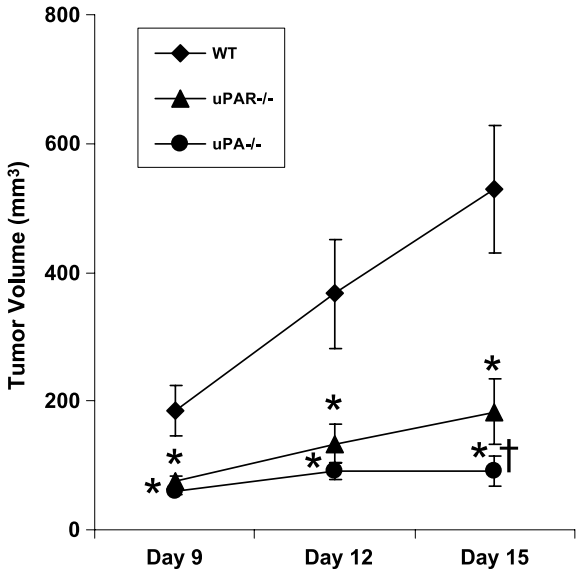

Figure 1. Effects of uPA or uPAR deficiency on murine prostate cancer RM-1 cell growth in mice. RM-1 cells were inoculated subcutaneously into the mice deficient either of uPA ($n = 10$) or uPAR ($n = 8$) and wild-type (WT) counterparts ($n = 8$). The tumor volume was measured in WT, uPA$^{-/-}$, and uPAR$^{-/-}$ mice on days 9, 12, and 15 after tumor cell inoculation. Values represent mean ± SD. *$P < .001$, compared with the tumor volume in WT mice. †$P < .05$, compared with the tumor volume in uPAR$^{-/-}$ mice.

Angiogenesis in Allograft Tumors Was Diminished in uPA$^{-/-}$ and uPAR$^{-/-}$ Mice Compared with the WT Animals

Excised allograft tumors were collected, and the tumor sections were stained for CD31 expression and analyzed. Figure 2*A* represents photographs of the tumors in these mice. Figure 2*B* demonstrates the quantitative measurement of vessel density in the excised tumors. A significant reduction in the number of blood vessels was identified in the allograft tumors from both uPA$^{-/-}$ and uPAR$^{-/-}$ mice compared with the tumors from WT mice (Figure 2).

Tumors in uPA$^{-/-}$ and uPAR$^{-/-}$ Mice Revealed Significantly Lower Proliferation and Higher Apoptotic Indices Compared with the Tumors in WT Animals

To determine the effects of uPA or uPAR deficiencies on prostate cancer cell proliferation and apoptosis *in vivo*, the tumor sections were stained for Ki-67 and ApopTag (Figure 3*A*). Quantitative analysis of the immunohistochemical staining revealed less Ki-67–positive cells and more ApopTag-positive cells in allograft tumors from both uPA$^{-/-}$ and uPAR$^{-/-}$ mice compared with the tumors from the WT mice (Figure 3*B*). In addition, uPA production in RM-1 cell culture conditioned medium was measured by ELISA. RM-1 cells produced a high amount of endogenous uPA at 53.7 ng/50,000 cells. RM-1 cells expressed both uPA and uPAR messenger RNA determined by reverse transcription–PCR (data not shown).

Tumors in uPA$^{-/-}$ and uPAR$^{-/-}$ Mice Displayed Significantly Less Infiltrating Macrophages (TAMs) Compared with the Tumors in WT Animals

To test whether host-derived uPA or uPAR contributes to the accumulation of TAMs in the allograft tumors, sections were stained with F4/80 antibody, which recognizes a cell surface glycoprotein specifically expressed in mature tissue macrophages [33]. There was significantly less F4/80-positive macrophage infiltration in allograft tumors from both uPA$^{-/-}$ and uPAR$^{-/-}$ mice compared with the tumors from WT mice (Figure 4*A*). Macrophage infiltration as measured by fluorescein isothiocyanate–conjugated antimouse MAC3 antibody by flow cytometry analysis was significantly reduced in the allograft tumors from both uPA$^{-/-}$ and uPAR$^{-/-}$ mice compared with the tumors from the WT mice (Figure 4*B*) [34]. These findings suggest a link between activation of the uPA/uPAR axis and macrophage infiltration in the tumor microenvironment. Because diminished RM-1 tumors in uPA$^{-/-}$ and uPAR$^{-/-}$ mice also suggest generation of systemic antitumor immunity, tumor-infiltrating lymphocytes, such as CD4$^+$ and CD8$^+$ cells, were examined. The number of CD8$^+$ cells, but not the number of CD4$^+$ cells, was significantly increased in uPA$^{-/-}$ allograft tumors compared with the uPAR$^{-/-}$ or the WT tumors (Figure 4*C*).

In Vitro *Macrophage Migration Was Inhibited in Both uPA$^{-/-}$ and uPAR$^{-/-}$ Mice Compared with the Control Mice*

To further investigate the roles of the uPA/uPAR axis in macrophage chemotaxis *in vitro*, peritoneal macrophages were collected from WT,

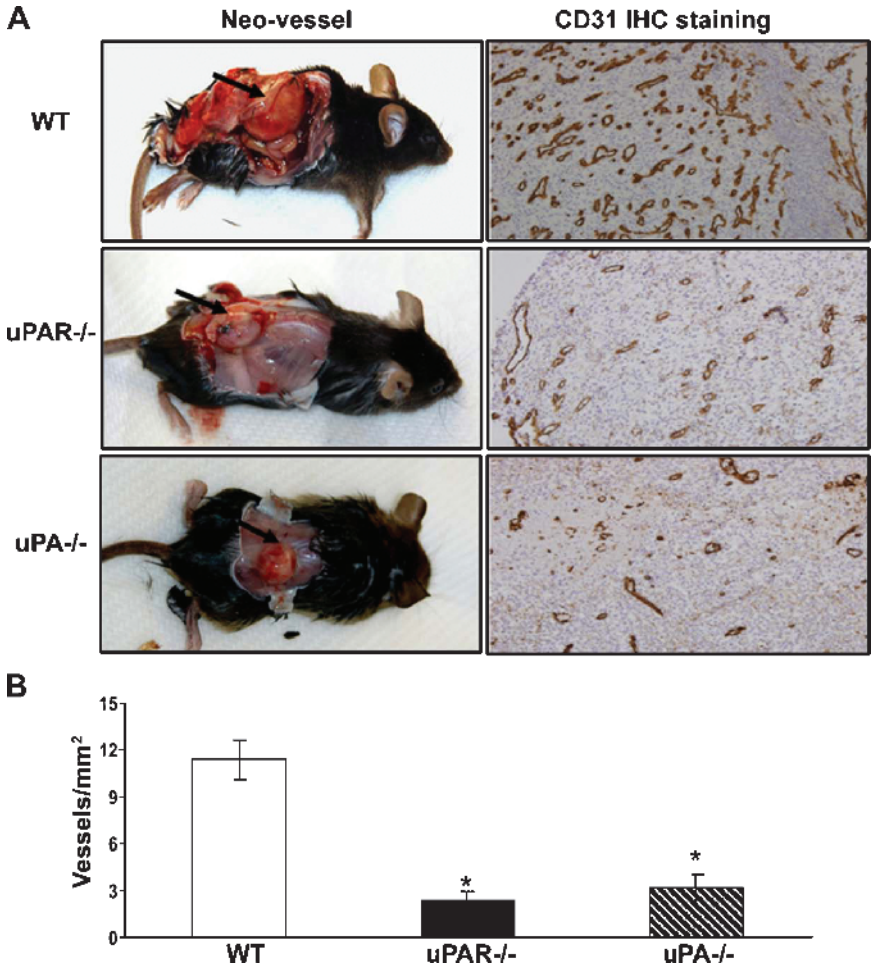

Figure 2. Effects of uPA or uPAR deficiency on RM-1 tumor angiogenesis. Tumors were excised from WT, uPA$^{-/-}$, and uPAR$^{-/-}$ mice on day 15 after tumor cell inoculation. (A) Representative photographs of tumor sizes and blood vessel formation. The excised tumor sections were stained with an antibody against endothelial marker CD31. (B) Quantified vessel density was determined by the number of vessels in five randomly selected fields (×200). Values represent mean ± SEM. *$P < .001$, compared with the number of vessels per squared millimeter in tumor sections from the WT mice.

uPA$^{-/-}$, and uPAR$^{-/-}$ mice and tested in an *in vitro* migration assay using conditioned medium collected from RM-1 cells. Macrophage chemotaxis was significantly diminished in the macrophages from both uPA$^{-/-}$ and uPAR$^{-/-}$ mice compared with the macrophages from the WT mice (Figure 5). As a positive control, recombinant mouse MCP-1 significantly induced macrophage chemotaxis (data not shown).

Discussion

The uPA/uPAR axis has been demonstrated to play a central role in prostate cancer tumorigenesis through direct and indirect interactions with integrins, endocytosis receptors, and growth factors in the tumor microenvironment (see review in Li and Cozzi [2]). The contribution of tumor-derived *versus* host-derived uPA on the tumor development remains unclear. In the current study, murine prostate cancer RM-1 cells were subcutaneously implanted into WT, uPA$^{-/-}$, and uPAR$^{-/-}$ mice. Tumor growth was dramatically diminished in both uPA$^{-/-}$ and uPAR$^{-/-}$ mice compared with WT control animals. Both tumor-derived and host-derived uPA contributed to prostate cancer growth *in vivo*. Tumors in uPA$^{-/-}$ and uPAR$^{-/-}$ mice displayed significantly less infiltrating TAMs compared with the tumors in WT animals. TAMs, derived from circulating monocytes, have been demonstrated to release a variety of growth factors, inflammatory mediators, and proteolytic enzymes in the tumor microenvironment. To our knowledge, this is the first report that demonstrates a direct link between activation of the uPA/uPAR axis and infiltrating TAMs in prostate cancer development. In addition, we observed that diminished RM-1 tumors in uPA$^{-/-}$ mice, but not in uPAR$^{-/-}$ mice, indeed were associated with enhanced tumor infiltrating lymphocytes, such as CD8^{+} cells, but not CD4^{+} T helper cells, suggesting that uPA also participates in intratumoral CD8^{+} T cell–mediated antitumor immunity. The enhanced tumor-infiltrating CD8^{+} cells in this model are independent of uPAR$^{-/-}$. However, further investigations on the roles of T regulatory cells and dendritic cells are needed.

uPA and uPAR are expressed in a variety of solid tumors including prostate, breast, colon, ovarian, renal, lung, liver, and pancreatic cancers, as well as hematological malignancies (see review in Smith and Marshall [1] and Mekkawy et al. [34]). In prostate cancer, up-regulation of the uPA and uPAR axis was identified not only in tumor epithelial cells but also in endothelial cells and macrophages but rarely in other nonmalignant cells (see review in Li and Cozzi [2]). In this study, we

demonstrated that RM-1 cells, expressing both uPA and uPAR, grew in $uPA^{-/-}$ and $uPAR^{-/-}$ mice. Furthermore, tumors in $uPA^{-/-}$ and $uPAR^{-/-}$ mice revealed significantly lower proliferation and higher apoptotic indices compared with the tumors in WT animals. This suggests that, in addition to paracrine effects, an autocrine axis indeed exists for the tumor cells themselves. Blood vessel density in allograft tumors was diminished in $uPA^{-/-}$ and $uPAR^{-/-}$ mice compared with the WT animals. This result is consistence with a prior report in a murine fibrosarcoma mouse model that demonstrated a reduction of tumor angiogenesis in $uPA^{-/-}$ mice [35].

A greater inhibition of the tumor growth in $uPA^{-/-}$ mice compared with $uPAR^{-/-}$ mice was observed. This suggests a possibly predominant contribution of stroma-derived uPA in the tumor development. It may further indicate that uPA may be required for cancer cell survival and

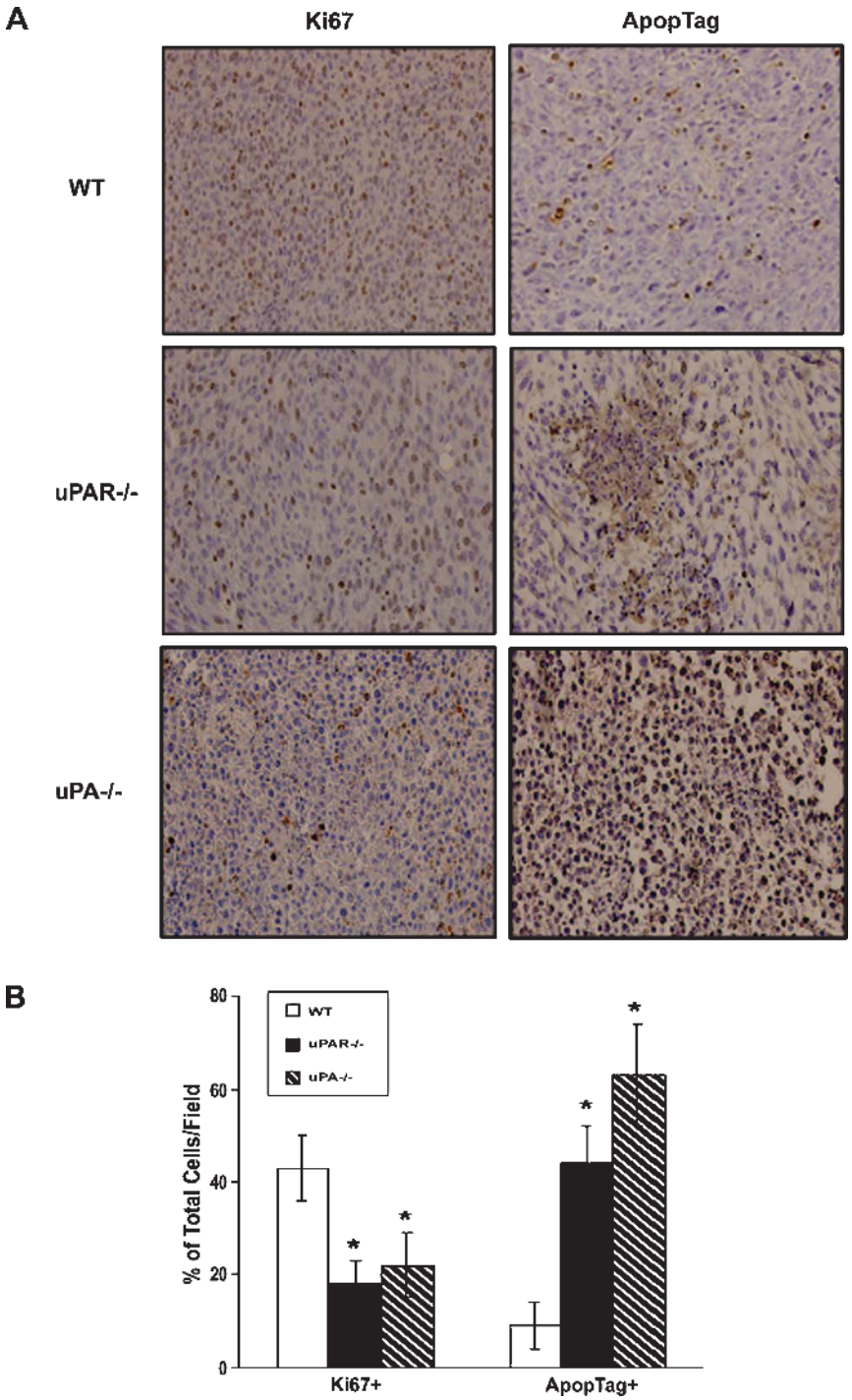

Figure 3. Effects of uPA or uPAR deficiency on RM-1 tumor cell proliferation and apoptosis. Tumor sections were immunohistochemically stained with Ki-67 monoclonal antibody or by an ApopTag *in situ* detection kit, respectively. (A) Representative photographs of immunohistochemical staining. (B) Quantified data were determined by the number of Ki-67–positive cells or the number of apoptotic-positive nuclei dividing the total number of cells in five randomly selected fields under light microscopy (×400). Values represent mean ± SEM. *$P <$ .001, compared with the percentage of positive cells in tumor sections from the WT mice.

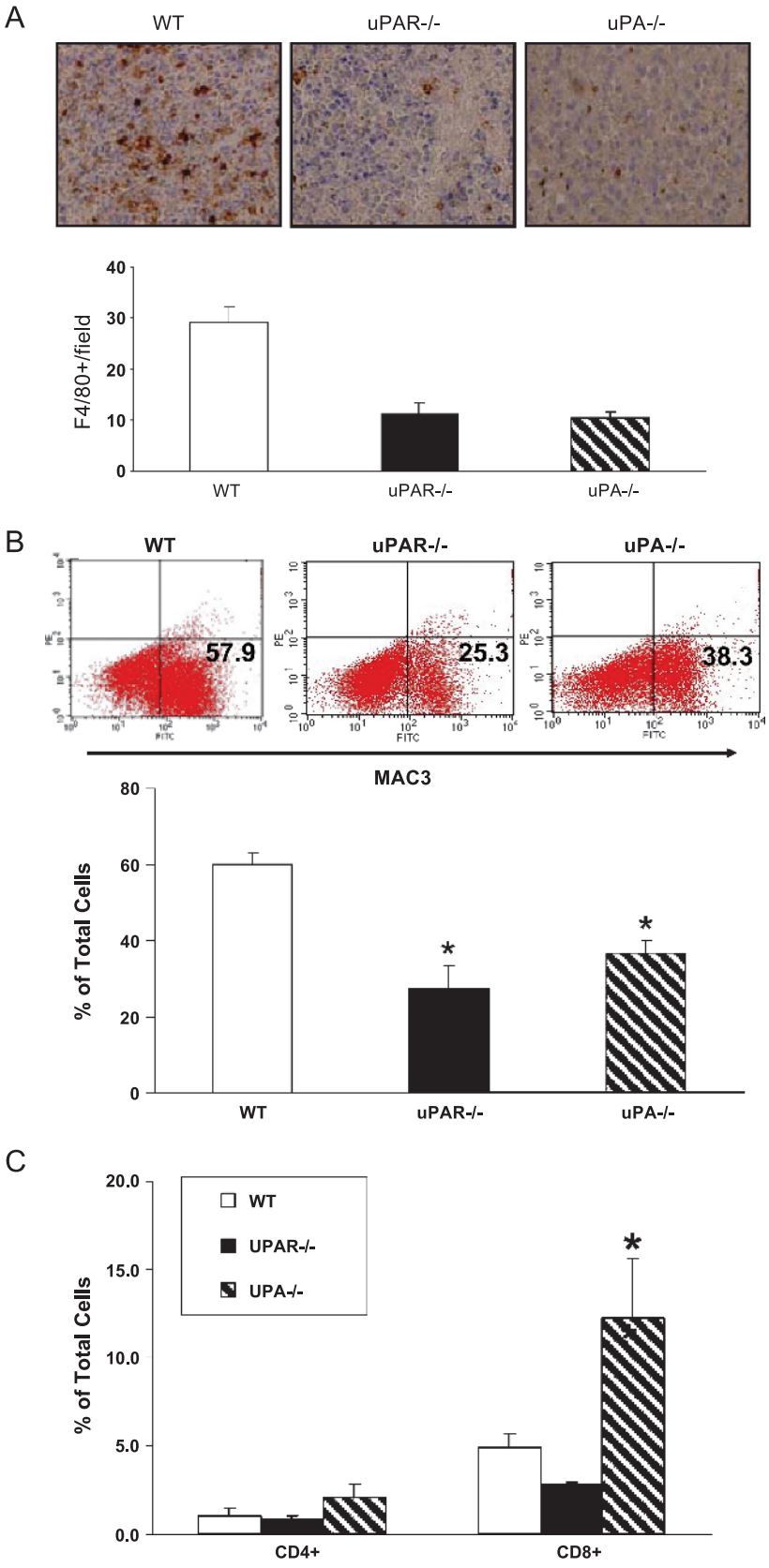

Figure 4. Effects of uPA or uPAR deficiency on TAMs infiltration. (A) Tumor sections were immunohistochemically stained with F4/80 monoclonal antibody. Representative results show macrophage infiltration into tumors and quantification of F4/80-positive mature macrophages. Values represent mean ± SEM. *$P < .001$, compared with the number of positive cells in tumor sections from the WT mice. (B) Representative results show the percentage of MAC3-positive cells from excised tumors analyzed by flow cytometry and quantified data on percentage of MAC3-positive cells. (C) Quantified data on CD4- and CD8-positive cells. Values represent mean ± SEM. *$P < .001$, compared with the percentage of positive cells in tumor allografts from the WT mice.

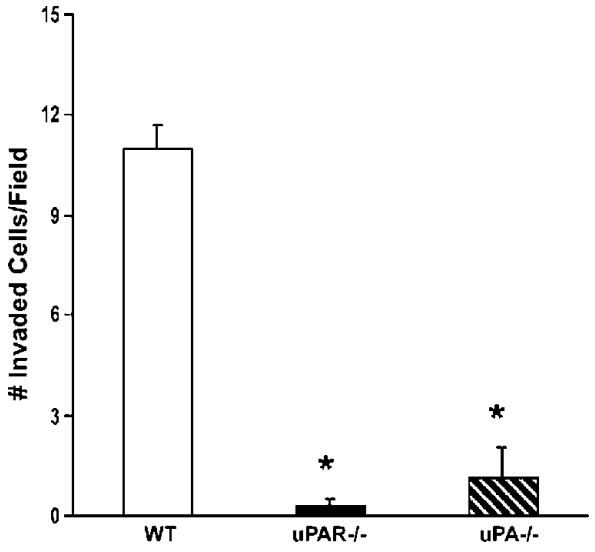

Figure 5. Effects of uPA or uPAR deficiency on macrophage chemotaxis *in vitro*. Peritoneal macrophages were collected from WT, $uPA^{-/-}$, and $uPAR^{-/-}$ mice. *In vitro* chemotaxis assays were performed using conditioned medium collected from RM-1 cells as described in Materials and Methods. Recombinant MCP-1 (10 ng/ml) were used a positive control. The number of migrated macrophages was counted. Values represent mean ± SEM. *$P < .001$, compared with the number of invaded macrophages from the WT mice.

proliferation in the tumor microenvironment. In $uPAR^{-/-}$ mice, with no uPAR expression in host cells, the RM-1 tumor cells grew at a significant lower rate compared with the tumor cell growth in WT mice. When there was no uPA production by the host environment in $uPA^{-/-}$ mice, the tumor-derived uPA was not enough to sustain the proliferating potential of the RM-1 cells. Production of stromal-derived uPA, therefore, plays a dominant role in the RM-1 tumor growth. It has been recently reported that overexpression of Notch 1 in prostate cancer promotes tumor invasion through induction of uPA and matrix metalloproteinase 9 [36] and that down-regulation of Notch 1 inhibits prostate cancer cell growth, migration, and invasion and induces apoptosis via inactivation of AKt, mammalian target of rapamycin, and nuclear factor κB signaling pathways [37]. Notch 1, a type 1 transmembrane protein, plays a key role in the development of many tissues and organ types. Aberrant Notch signaling, found in a wide variety of human cancers including prostate cancer, contributes to tumor development. Notch 1, therefore, may dictate uPA/uPAR signaling alterations in cancer stem cell survival and differentiation. Further studies on the roles of Notch 1 on uPA/uPAR signaling in prostate cancer stem cell pathobiology are warranted.

In conclusion, this study differentiates the major source of uPA in the tumor microenvironment as stromal-derived. The uPA/uPAR axis remains an interesting target for cancer therapy, directed at cancer cells as well as supporting host stromal cells.

Acknowledgments

The authors thank B. Rice for his technical assistance and K.A. Hassan and H. Roca for their helpful discussions.

References

[1] Smith HW and Marshall CJ (2010). Regulation of cell signalling by uPAR. *Nat Rev Mol Cell Biol* **11**, 23–36.

[2] Li Y and Cozzi PJ (2007). Targeting uPA/uPAR in prostate cancer. *Cancer Treat Rev* **33**, 521–527.

[3] Duffy MJ (1990). Plasminogen activators and cancer. *Blood Coagul Fibrinolysis* **1**, 681–687.

[4] Grondahl-Hansen J, Agerlin N, Munkholm-Larsen P, Bach F, Nielsen LS, Dombernowsky P, and Dano K (1988). Sensitive and specific enzyme-linked immunosorbent assay for urokinase-type plasminogen activator and its application to plasma from patients with breast cancer. *J Lab Clin Med* **111**, 42–51.

[5] Hasui Y, Marutsuka K, Suzumiya J, Kitada S, Osada Y, and Sumiyoshi A (1992). The content of urokinase-type plasminogen activator antigen as a prognostic factor in urinary bladder cancer. *Int J Cancer* **50**, 871–873.

[6] Nishino N, Aoki K, Tokura Y, Sakaguchi S, Takada Y, and Takada A (1988). The urokinase type of plasminogen activator in cancer of digestive tracts. *Thromb Res* **50**, 527–535.

[7] Miyake H, Hara I, Yamanaka K, Gohji K, Arakawa S, and Kamidono S (1999). Elevation of serum levels of urokinase-type plasminogen activator and its receptor is associated with disease progression and prognosis in patients with prostate cancer. *Prostate* **39**, 123–129.

[8] Shariat SF, Roehrborn CG, McConnell JD, Park S, Alam N, Wheeler TM, and Slawin KM (2007). Association of the circulating levels of the urokinase system of plasminogen activation with the presence of prostate cancer and invasion, progression, and metastasis. *J Clin Oncol* **25**, 349–355.

[9] Lilja H, Vickers A, and Scardino P (2007). Measurements of proteases or protease system components in blood to enhance prediction of disease risk or outcome in possible cancer. *J Clin Oncol* **25**, 347–348.

[10] Miyake H, Hara I, Yamanaka K, Arakawa S, and Kamidono S (1999). Elevation of urokinase-type plasminogen activator and its receptor densities as new predictors of disease progression and prognosis in men with prostate cancer. *Int J Oncol* **14**, 535–541.

[11] Van Veldhuizen PJ, Sadasivan R, Cherian R, and Wyatt A (1996). Urokinase-type plasminogen activator expression in human prostate carcinomas. *Am J Med Sci* **312**, 8–11.

[12] Gavrilov D, Kenzior O, Evans M, Calaluce R, and Folk WR (2001). Expression of urokinase plasminogen activator and receptor in conjunction with the ets family and AP-1 complex transcription factors in high grade prostate cancers. *Eur J Cancer* **37**, 1033–1040.

[13] Usher PA, Thomsen OF, Iversen P, Johnsen M, Brunner N, Hoyer-Hansen G, Andreasen P, Dano K, and Nielsen BS (2005). Expression of urokinase plasminogen activator, its receptor and type-1 inhibitor in malignant and benign prostate tissue. *Int J Cancer* **113**, 870–880.

[14] Cozzi PJ, Wang J, Delprado W, Madigan MC, Fairy S, Russell PJ, and Li Y (2006). Evaluation of urokinase plasminogen activator and its receptor in different grades of human prostate cancer. *Hum Pathol* **37**, 1442–1451.

[15] Pulukuri SM, Estes N, Patel J, and Rao JS (2007). Demethylation-linked activation of urokinase plasminogen activator is involved in progression of prostate cancer. *Cancer Res* **67**, 930–939.

[16] Pulukuri SM, Gondi CS, Lakka SS, Jutla A, Estes N, Gujrati M, and Rao JS (2005). RNA interference–directed knockdown of urokinase plasminogen activator and urokinase plasminogen activator receptor inhibits prostate cancer cell invasion, survival, and tumorigenicity *in vivo*. *J Biol Chem* **280**, 36529–36540.

[17] Dong Z, Saliganan AD, Meng H, Nabha SM, Sabbota AL, Sheng S, Bonfil RD, and Cher ML (2008). Prostate cancer cell–derived urokinase-type plasminogen activator contributes to intraosseous tumor growth and bone turnover. *Neoplasia* **10**, 439–449.

[18] Gyetko MR, Todd RF III, Wilkinson CC, and Sitrin RG (1994). The urokinase receptor is required for human monocyte chemotaxis *in vitro*. *J Clin Invest* **93**, 1380–1387.

[19] Bryer SC, Fantuzzi G, Van Rooijen N, and Koh TJ (2008). Urokinase-type plasminogen activator plays essential roles in macrophage chemotaxis and skeletal muscle regeneration. *J Immunol* **180**, 1179–1188.

[20] Sica A, Schioppa T, Mantovani A, and Allavena P (2006). Tumour-associated macrophages are a distinct M2 polarised population promoting tumour progression: potential targets of anti-cancer therapy. *Eur J Cancer* **42**, 717–727.

[21] Balkwill F and Mantovani A (2001). Inflammation and cancer: back to Virchow? *Lancet* **357**, 539–545.

[22] Coussens LM and Werb Z (2002). Inflammation and cancer. *Nature* **420**, 860–867.

[23] Solinas G, Germano G, Mantovani A, and Allavena P (2009). Tumor-associated macrophages (TAM) as major players of the cancer-related inflammation. *J Leukoc Biol* **86**, 1065–1073.

[24] Kubo H, Morgenstern D, Quinian WM, Ward PA, Dinauer MC, and Doerschuk CM (1996). Preservation of complement-induced lung injury in mice with deficiency of NADPH oxidase. *J Clin Invest* **97**, 2680–2684.

[25] Carmeliet P, Schoonjans L, Kieckens L, Ream B, Degen J, Bronson R, De Vos R, van den Oord JJ, Collen D, and Mulligan RC (1994). Physiological consequences of loss of plasminogen activator gene function in mice. *Nature* **368**, 419–424.

[26] Dewerchin M, Nuffelen AV, Wallays G, Bouche A, Moons L, Carmeliet P, Mulligan RC, and Collen D (1996). Generation and characterization of urokinase receptor–deficient mice. *J Clin Invest* **97**, 870–878.

[27] Gyetko MR, Chen GH, McDonald RA, Goodman R, Huffnagle GB, Wilkinson CC, Fuller JA, and Toews GB (1996). Urokinase is required for the pulmonary inflammatory response to *Cryptococcus neoformans*. A murine transgenic model. *J Clin Invest* **97**, 1818–1826.

[28] Thompson TC, Southgate J, Kitchener G, and Land H (1989). Multistage carcinogenesis induced by *ras* and *myc* oncogenes in a reconstituted organ. *Cell* **56**, 917–930.

[29] Baley PA, Yoshida K, Qian W, Sehgal I, and Thompson TC (1995). Progression to androgen insensitivity in a novel *in vitro* mouse model for prostate cancer. *J Steroid Biochem Mol Biol* **52**, 403–413.

[30] Lu Y, Nie D, Witt WT, Chen Q, Shen M, Xie H, Lai L, Dai Y, and Zhang J (2008). Expression of the *fat-1* gene diminishes prostate cancer growth *in vivo* through enhancing apoptosis and inhibiting GSK-3 β phosphorylation. *Mol Cancer Ther* **7**, 3203–3211.

[31] Kindzelskii AL, Amhad I, Keller D, Zhou MJ, Haugland RP, Garni-Wagner BA, Gyetko MR, Todd RF III, and Petty HR (2004). Pericellular proteolysis by leukocytes and tumor cells on substrates: focal activation and the role of urokinase-type plasminogen activator. *Histochem Cell Biol* **121**, 299–310.

[32] Power CA, Pwint H, Chan J, Cho J, Yu Y, Walsh W, and Russell PJ (2009). A novel model of bone-metastatic prostate cancer in immunocompetent mice. *Prostate* **69**, 1613–1623.

[33] Austyn JM and Gordon S (1981). F4/80, a monoclonal antibody directed specifically against the mouse macrophage. *Eur J Immunol* **11**, 805–815.

[34] Mekkawy AH, Morris DL, and Pourgholami MH (2009). Urokinase plasminogen activator system as a potential target for cancer therapy. *Future Oncol* **5**, 1487–1499.

[35] Gutierrez LS, Schulman A, Brito-Robinson T, Noria F, Ploplis VA, and Castellino FJ (2000). Tumor development is retarded in mice lacking the gene for urokinase-type plasminogen activator or its inhibitor, plasminogen activator inhibitor-1. *Cancer Res* **60**, 5839–5847.

[36] Bin Hafeez B, Adhami VM, Asim M, Siddiqui IA, Bhat KM, Zhong W, Saleem M, Din M, Setaluri V, and Mukhtar H (2009). Targeted knockdown of Notch1 inhibits invasion of human prostate cancer cells concomitant with inhibition of matrix metalloproteinase-9 and urokinase plasminogen activator. *Clin Cancer Res* **15**, 452–459.

[37] Wang Z, Li Y, Banerjee S, Kong D, Ahmad A, Nogueira V, Hay N, and Sarkar FH (2010). Down-regulation of Notch-1 and Jagged-1 inhibits prostate cancer cell growth, migration and invasion, and induces apoptosis via inactivation of Akt, mTOR, and NF-κB signaling pathways. *J Cell Biochem* **109**, 726–736.